Electronic Supplementary Material (ESI) for Journal of Materials Chemistry A.
This journal is © The Royal Society of Chemistry 2018

Electronic supplementary information

Boosting Solid-state Flexible Supercapacitors by Employing Tailored Hierarchical Carbon Electrodes and High-voltage Organic Gel Electrolyte

Wenhao Liu,[a, c] Kai Wang,* [a, b] , Chen Li, [a, b] Xiong Zhang, [a, b] Xianzhong Sun, [a, b] Jianwei Han, [a, b] Xing-long Wu,* [c] Feng Li* [d] and Yanwei Ma* [a, b]

[a.] *Institute of Electrical Engineering, Chinese Academy of Sciences, Beijing 100190, P.R. China*

[b.] *University of Chinese Academy of Sciences, Beijing 100049, PR China*

[c.] *National & Local United Engineering Laboratory for Power Batteries, Faculty of Chemistry, Northeast Normal University, Changchun, Jilin 130024, P. R. China*

[d.] *Shenyang National Laboratory for Materials Science, Institute of Metal Research, Chinese Academy of Science, 72 Wenhua Road, Shenyang 110016, China*

*E-mail: wangkai@mail.iee.ac.cn; ywma@mail.iee.ac.cn; xinglong@nenu.edu.cn; fli@imr.ac.cn

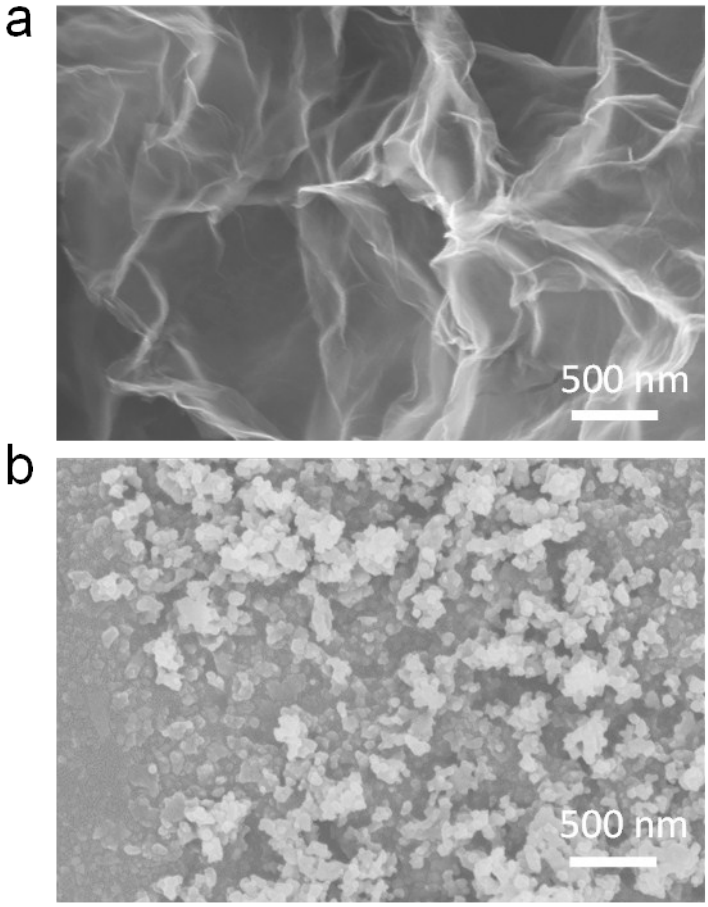

Figure S1. SEM images of a) pristine graphene oxide and b) ZIF-8 polyhedrons.

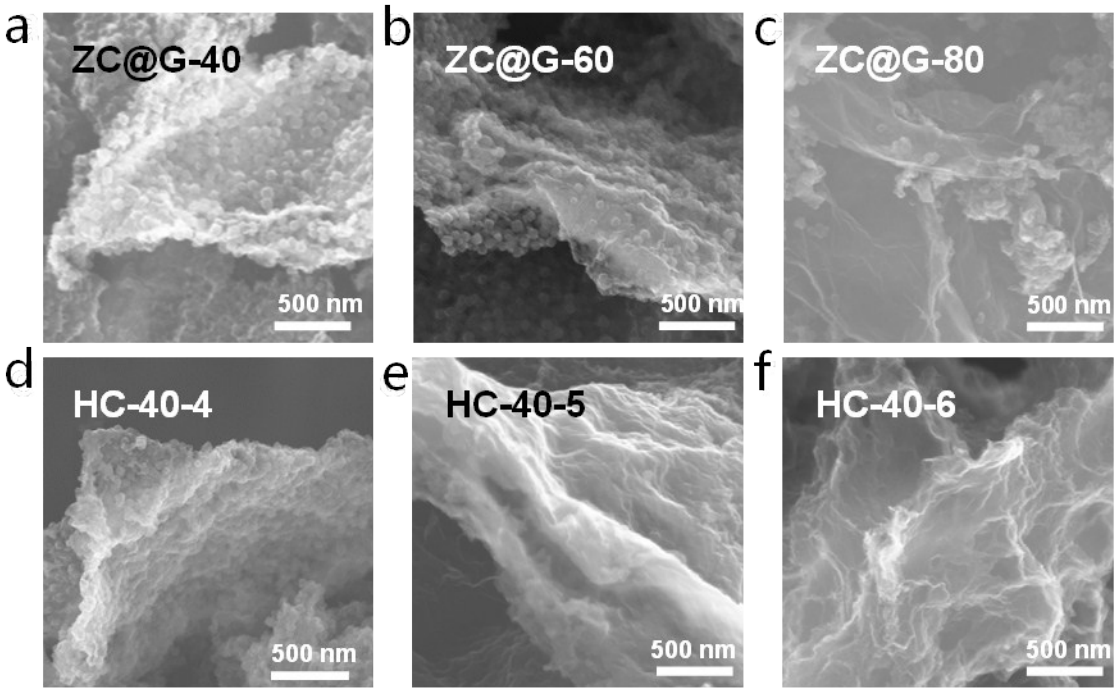

Figure S2. SEM images of a) ZC@G-40, b) ZC@G-60, c) ZC@G-80, d) HC-40-4, e) HC-40-5 and f) HC-40-6.

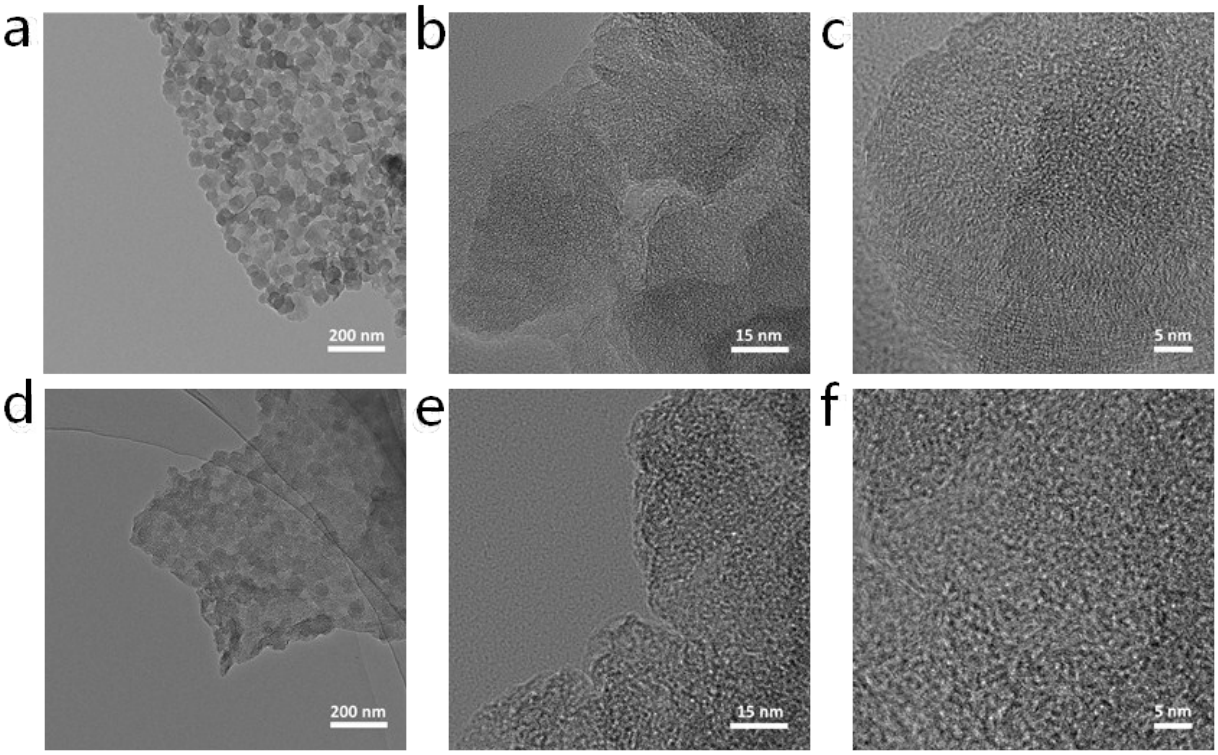

Figure S3. TEM and HRTEM images of a-c) ZC@G-40 and d-f) HC-40-4 with various magnifications.

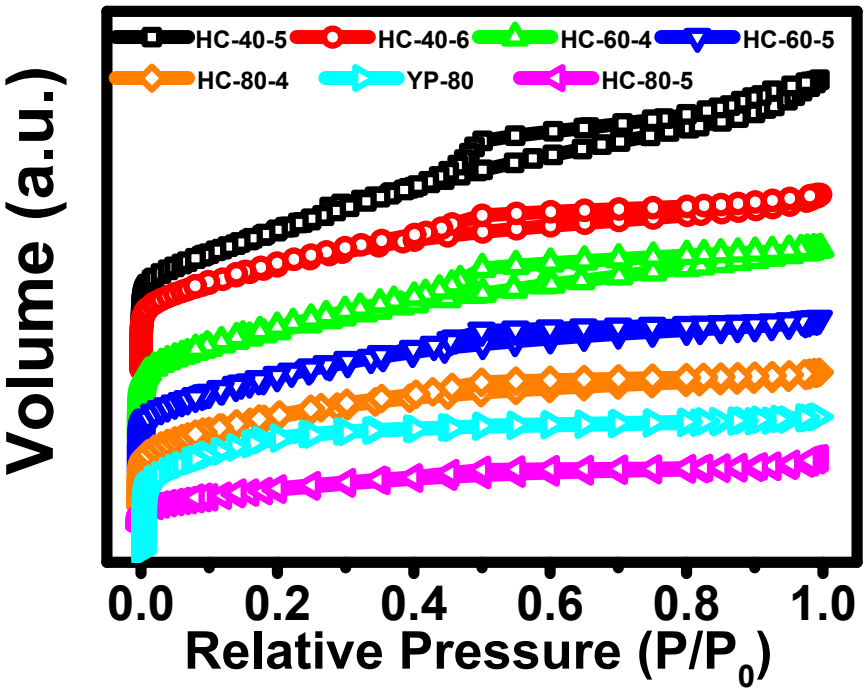

Figure S4. N_2 adsorption–desorption isotherms of samples prepared with different GO or KOH amount and YP-80.

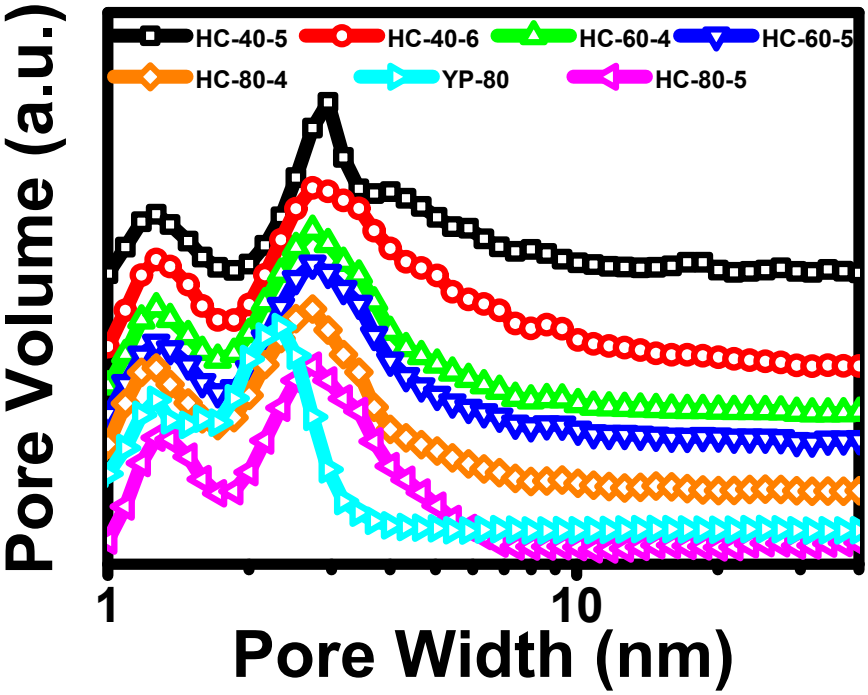

Figure S5. Pore size distribution of corresponding samples obtained by different conditions.

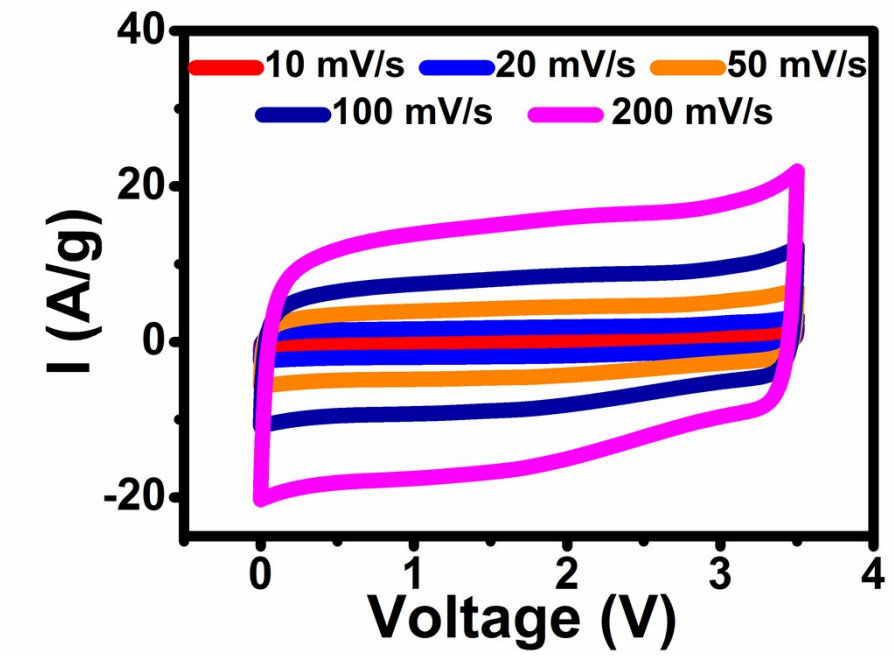

Figure S6. CV curves of HC-40-4 sample at various scanning rates.

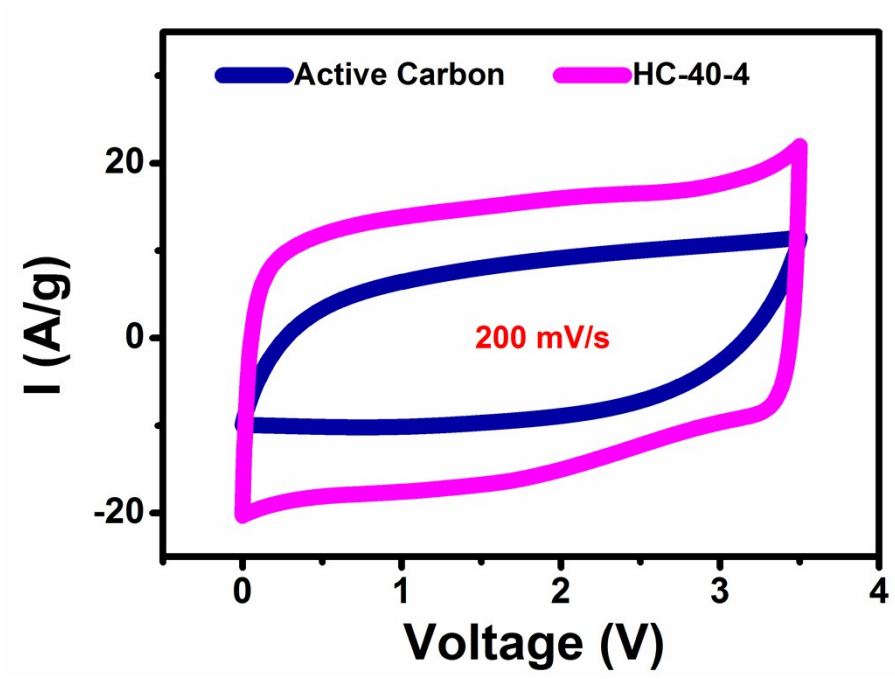

Figure S7. CV curves of HC-40-4 sample compared with commercial active carbon at 200 mV/s.

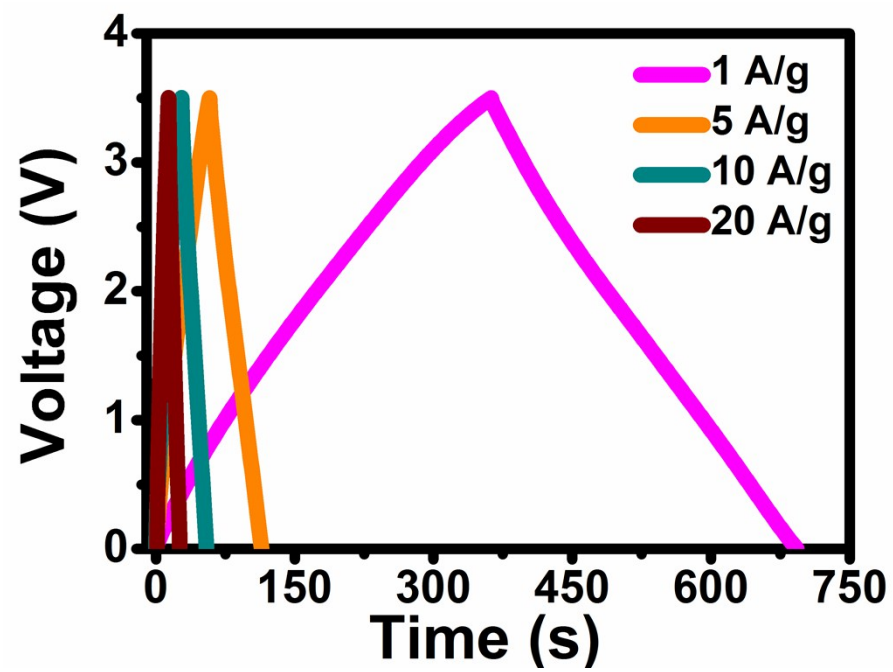

Fig S8. Galvanostatic charge/discharge profile of HC-40-4 electrode under different current densities.

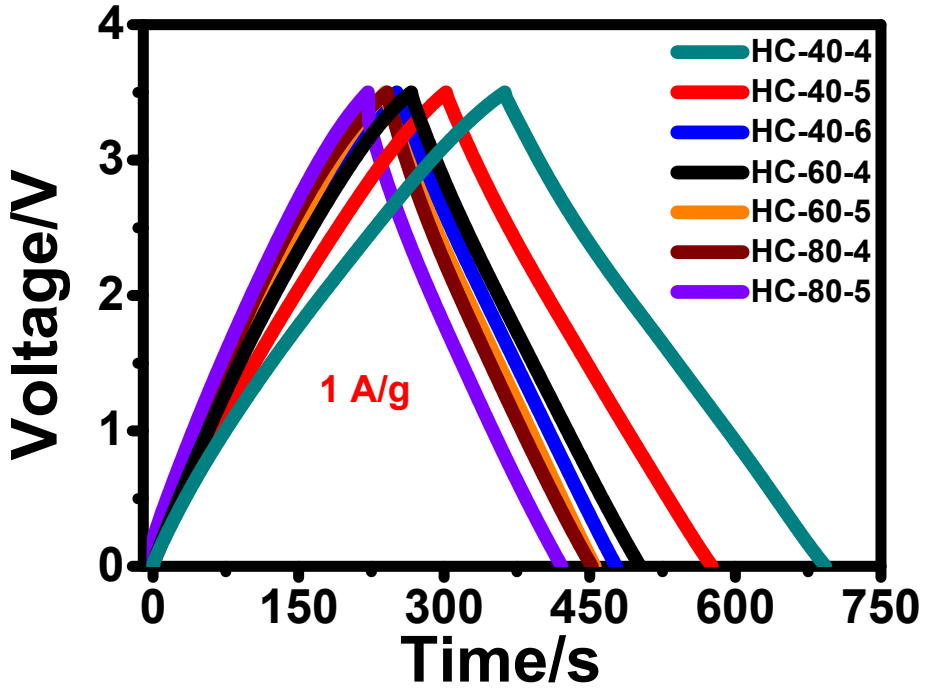

Figure S9. Galvanostatic charge/discharge profiles of various samples synthesized under different conditions.

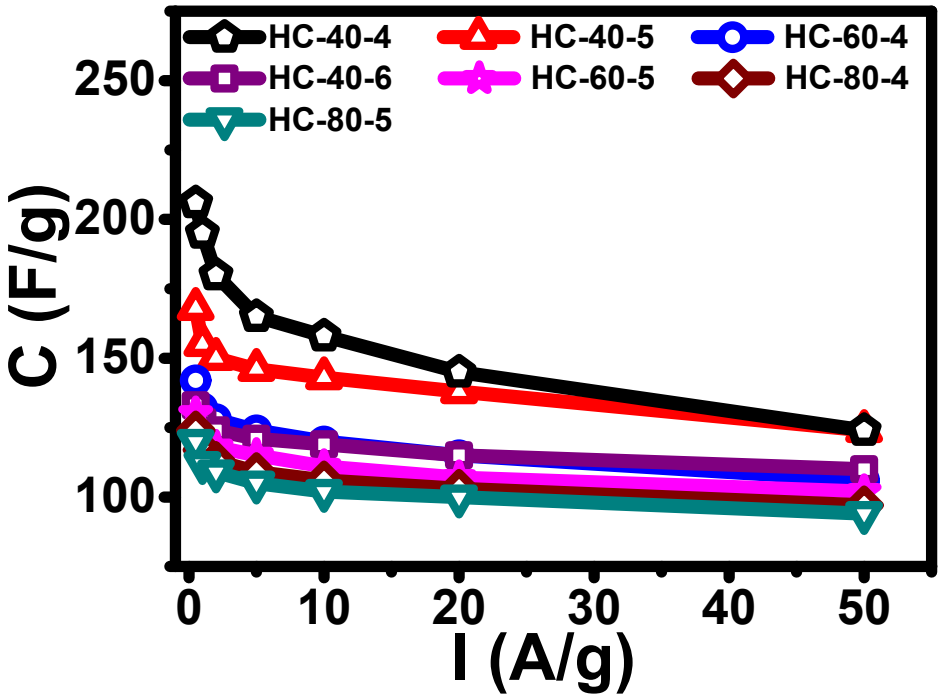

Figure S10. Specific capacitance of HC-x-y electrodes at various current densities.

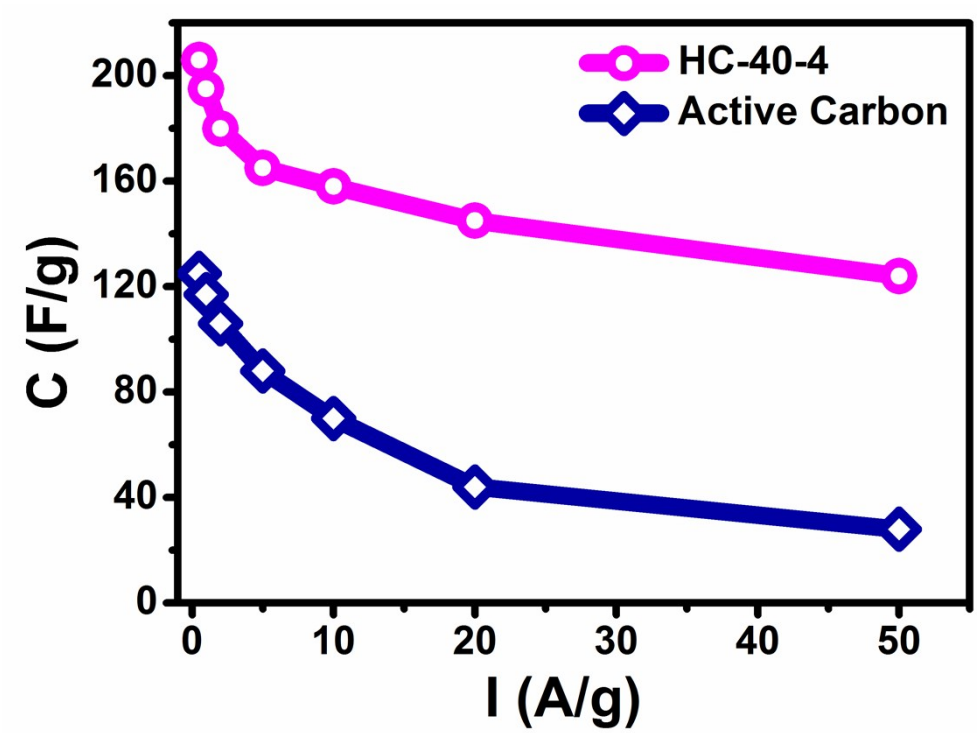

Figure S11. Specific capacitance of HC-40-4 and commercial active carbon.

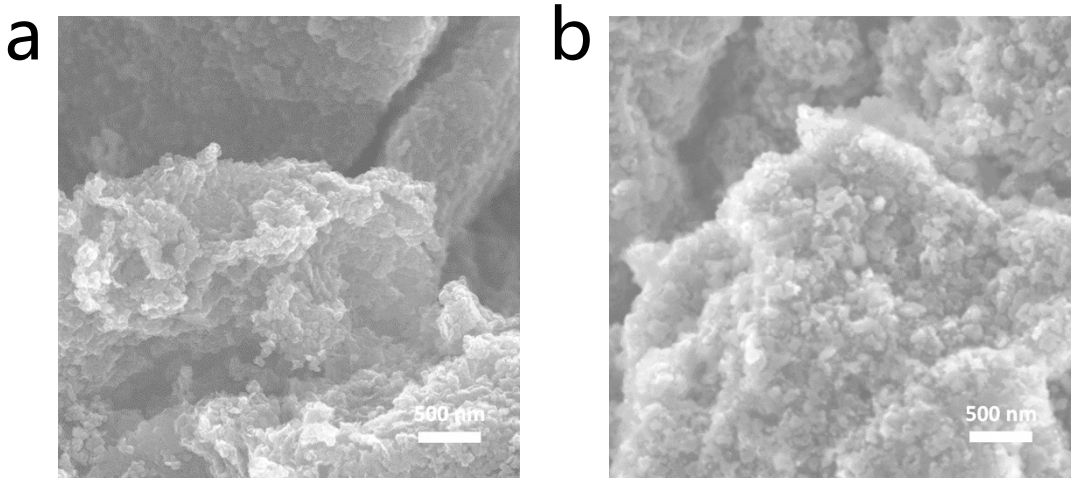

Figure S12. SEM images of HC-40-4 electrode a) before and b) after 10000 cycles at 50 A/g.

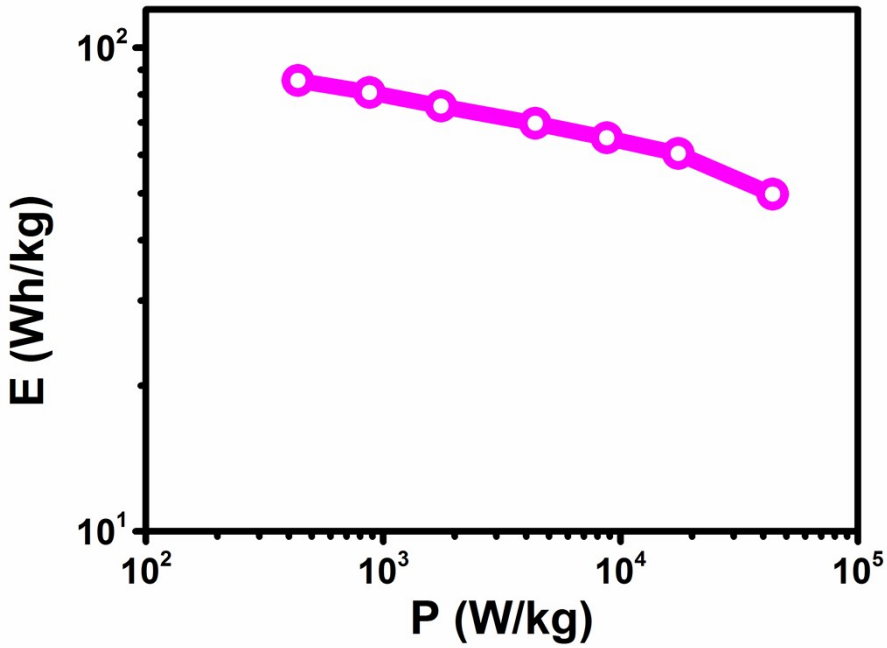

Figure S13. Ragone plots of the flexible device fabricated with HC-40-4 electrode and ionic liquid based gel electrolyte.

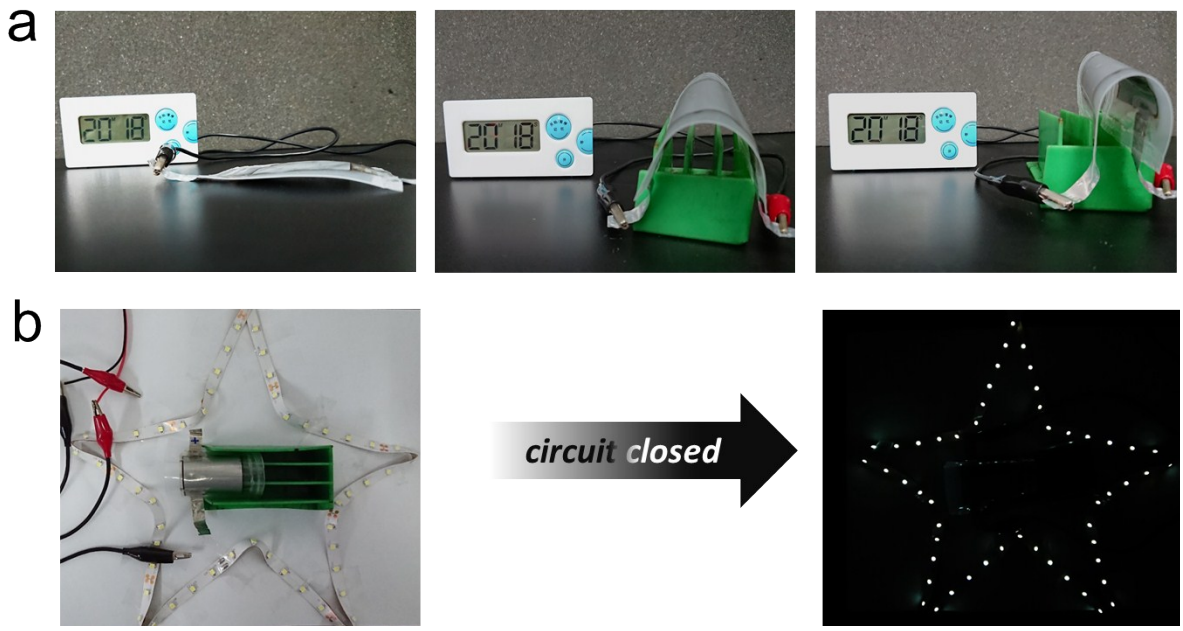

Figure S14. Photos of a) electric timer powered by flexible supercapacitor under different bending angles and b) pentacle-shaped LED string lighted by bended flexible device.

Table S1. Pore structures and conductivity properties of various materials.

Material	SSA (m^2/g)	Pore size (nm)	Total pore volume (cm^3/g)	Electrical conductivity (S/m)
PrGO	231	10.66	0.36	7692
ZC@G-40	1092	2.35	0.75	6752
HC-40-4	2837	3.03	2.12	6678
HC-40-5	2684	3.61	2.60	6564
HC-40-6	2020	3.27	1.58	——
HC-60-4	2077	3.08	1.46	6887
HC-60-5	1980	2.90	1.32	6791
HC-80-4	1807	3.14	1.15	7155
HC-80-5	1782	2.84	1.07	7049

Table S2. XPS elemental analysis of ZIF-8@GO nanocomposites, ZC@G-40 and HC-40-4 samples, respectively.

Material	C content (Atom %)	O content (Atom %)	N content (Atom %)	Zn content (Atom %)
ZIF-8@GO	60.33	5.69	25.68	8.31
ZC@G-40	79.94	5	13.75	1.3
HC-40-4	87.85	9.68	2.41	0.16